J|A|C|S
ARTICLES
Published on Web 01/27/2004

Intramolecular Charge Transfer with the Planarized 4-Aminobenzonitrile 1-*tert*-Butyl-6-cyano-1,2,3,4-tetrahydroquinoline (NTC6)

Klaas A. Zachariasse,*,† Sergey I. Druzhinin,† Wilfried Bosch,† and Reinhard Machinek‡

Contribution from the Max-Planck-Institut für Biophysikalische Chemie, Spektroskopie und Photochemische Kinetik, 37070 Göttingen, Germany, and Institut für Organische Chemie, Universität Göttingen, Tammannstrasse 2, 37077 Göttingen, Germany

Received July 25, 2003; E-mail: kzachar@gwdg.de

Abstract: Fast and efficient intramolecular charge transfer (ICT) and dual fluorescence is observed with the planarized aminobenzonitrile 1-*tert*-butyl-6-cyano-1,2,3,4-tetrahydroquinoline (NTC6) in a series of solvents from *n*-hexane to acetonitrile and methanol. Such a reaction does not take place for the related molecules with 1-isopropyl (NIC6) and 1-methyl (NMC6) groups, nor with the 1-alkyl-5-cyanoindolines with methyl (NMC5), isopropyl (NIC5), or *tert*-butyl (NTC5) substituents. For these molecules, a single fluorescence band from a locally excited (LE) state is found. The charge transfer reaction of NTC6 is favored by its relatively small energy gap $\Delta E(S_1,S_2)$, in accordance with the PICT model for ICT in aminobenzonitriles. For the ICT state of NTC6, a dipole moment of around 19 D is obtained from solvatochromic measurements, similar to μ_e(ICT) = 17 D of 4-(dimethylamino)benzonitrile (DMABN). For NMC5, NIC5, NTC5, NMC6, and NIC6, a dipole moment of around 10 D is determined by solvatochromic analysis, the same as that of the LE state of DMABN. For NTC6 in diethyl ether at −70 °C, the forward ICT rate constant (1.3×10^{11} s^{-1}) is much smaller than that of the back reaction (5.9×10^{9} s^{-1}), showing that the equilibrium is on the ICT side. The results presented here make clear that ICT can very well take place with a planarized molecule such as NTC6, when $\Delta E(S_1,S_2)$ is sufficiently small, indicating that a perpendicular twist of the amino group relative to the rest of the molecule is not necessary for reaching an ICT state with a large dipole moment. The six-membered alicyclic ring in NMC6, for example, prevents ICT by increasing $\Delta E(S_1,S_2)$ relative to that of DMABN.

Introduction

In the investigation of intramolecular charge transfer (ICT) with dual fluorescent electron donor(D)/acceptor(A)-substituted aromatic hydrocarbons such as 4-(dimethylamino)benzonitrile (DMABN), the molecular structure of the ICT state is an important point of discussion.[1−7] In the twisted intramolecular charge transfer (TICT) model,[8−10] it is postulated that the dimethylamino group of DMABN and its derivatives undergoes a twist of 90° relative to the benzonitrile moiety, from a coplanar configuration in LE to a mutually perpendicular structure in the ICT state. The planar intramolecular charge transfer (PICT) model,[7,11−13] on the other hand, assumes that the ICT state of DMABN is largely planar.[14−16] In this model, the magnitude of the energy gap $\Delta E(S_1,S_2)$ between the two lowest excited singlet states plays a crucial role.[7]

Until the advent of direct methods to determine excited-state structures, such as picosecond X-ray analysis,[17,18] planarized derivatives of DMABN fixed by a methylene bridge between

† Max-Planck-Institut für Biophysikalische Chemie.
‡ Universität Göttingen.

(1) Ma, C.; Kwok, W. M.; Matousek, P.; Parker, A. W.; Phillips, D.; Toner, W. T.; Towrie, M. *J. Phys. Chem. A* **2002**, *106*, 3294 and references cited therein.
(2) Okamoto, H.; Inishi, H.; Nakamura, Y.; Kohtani, S.; Nakagaki, R. *J. Phys. Chem. A.* **2001**, *105*, 4182.
(3) Okamoto, H.; Kinoshita, M.; Kohtani, S.; Nakagaki, R.; Zachariasse, K. A. *Bull. Chem. Soc. Jpn.* **2002**, *75*, 957.
(4) Zilberg, S.; Haas, Y. *J. Phys. Chem. A* **2002**, *106*, 1.
(5) Dobkowski, J.; Wójcik, J.; Koźminski, W.; Kołos, R.; Waluk, J.; Michl, J. *J. Am. Chem. Soc.* **2002**, *124*, 2406.
(6) Rettig, W.; Bliss, B.; Dirnberger, K. *Chem. Phys. Lett.* **1999**, *305*, 8.
(7) Zachariasse, K. A. *Chem. Phys. Lett.* **2000**, *320*, 8.
(8) Grabowski, Z. R.; Rotkiewicz, K.; Siemiarczuk, A.; Cowley, D. J.; Baumann, W. *Nouv. J. Chim.* **1979**, *3*, 443.
(9) Rettig, W. *Angew. Chem., Int. Ed. Engl.* **1986**, *25*, 971.
(10) Rettig, W. In *Topics in Current Chemistry, Electron-Transfer I*; Mattay, J., Ed.; Springer: Berlin, 1994; Vol. 169, p 253.
(11) Il'ichev, Yu. V.; Kühnle, W.; Zachariasse, K. A. *J. Phys. Chem. A* **1998**, *102*, 5670.
(12) Zachariasse, K. A.; Grobys, M.; von der Haar, Th.; Hebecker, A.; Il'ichev, Yu. V.; Jiang, Y.-B.; Morawski, O.; Kühnle, W. *J. Photochem. Photobiol., A: Chem.* **1996**, *102*, 59. Erratum: *J. Photochem. Photobiol., A: Chem.* **1998**, *115*, 259.
(13) Zachariasse, K. A.; Grobys, M.; von der Haar, Th.; Hebecker, A.; Il'ichev, Yu. V.; Morawski, O.; Rückert, I.; Kühnle, W. *J. Photochem. Photobiol., A: Chem.* **1997**, *105*, 373.
(14) The use of the name LE state in the ICT reaction of D/A-substituted molecules such as DMABN obviously originates from the formal kinetic similarity of the ICT reaction scheme consisting of an initially excited LE state and an ICT state (Scheme 1) and the schemes applicable to excimer and exciplex formation.
(15) Heine, A.; Herbst-Irmer, R.; Stalke, D.; Kühnle, W.; Zachariasse, K. A. *Acta Crystallogr.* **1994**, *B50*, 363.
(16) Berden, G.; van Rooy, J.; Meerts, W. L.; Zachariasse, K. A. *Chem. Phys. Lett.* **1997**, *278*, 373.
(17) Techert, S.; Schotte, F.; Wulff, M. *Phys. Rev. Lett.* **2001**, *86*, 2030.
(18) Techert, S.; Zachariasse, K. A. *J. Am. Chem. Soc.*, submitted.

the amino nitrogen and the benzene ring have played a major role in the investigations aimed at the elucidation of the ICT structure.[8−10,13,19−25] The first example of a model compound for a planar LE state that cannot form a TICT state was 1-methyl-5-cyanoindoline (NMC5).[24] Later, 1-methyl-6-cyano-1,2,3,4-tetrahydroquinoline (NMC6)[23] and 1-ethyl-5-cyanoindoline (NEC5)[21] were introduced as other model substances for LE.

With NMC5, NEC5, and NMC6, dual fluorescence was not observed: even in the strongly polar solvents acetonitrile and methanol, the fluorescence spectrum consists of a single LE band.[22−24] The absence of ICT fluorescence in the case of model compounds such as NMC6 was considered to be the most convincing evidence for the TICT model.[8−10,26]

A closer inspection of the absorption spectra of NMC5 and especially NMC6 reveals, however, that the planarization of these compounds by incorporating the amino nitrogen into an alicyclic ring results in a larger energy gap $\Delta E(S_1,S_2)$ as compared with more flexible aminobenzonitriles such as DMABN.[13] ICT does not take place with molecules having relatively large values for $\Delta E(S_1,S_2)$, such as with 4-(methylamino)benzonitrile (MABN), 4-aminobenzonitrile (ABN), and 4-(dimethylamino) phenylacetylene.[7,12,13,27−29] In support of the PICT model, fast and efficient ICT was observed with the planarized aminobenzonitrile 1-methyl-7-cyano-2,3,4,5-tetrahydro-1*H*-1-benzazepine (NMC7) in diethyl ether and acetonitrile.[12,13] For this molecule NMC7 with a seven-membered alicyclic ring, the $\Delta E(S_1,S_2)$ value is smaller than that for NMC6.

The replacement of the methyl substituents in DMABN, giving 4-(diisopropylamino)benzonitrile (DIABN), leads to a reduction of $\Delta E(S_1,S_2)$ and a strong increase in the efficiency of the ICT reaction results, to such an extent that ICT and dual fluorescence occur in the nonpolar solvent *n*-hexane, in the crystalline state, and even in the gas phase.[30−32] On the basis of the observed enhancement of the ICT efficiency by replacing methyl with isopropyl amino substituents, it was therefore attempted to synthesize derivatives of NMC5 and NMC6 with isopropyl and *tert*-butyl groups instead of methyl. Results obtained with these molecules, 1-isopropyl-5-cyanoindoline (NIC5), 1-isopropyl-6-cyano-1,2,3,4-tetrahydroquinoline (NIC6), 1-*tert*-butyl-5-cyanoindoline (NTC5), and 1-*tert*-butyl-6-cyano-1,2,3,4-tetrahydroquinoline (NTC6), are reported in this paper (Chart 1). For comparison, the 1-methyl derivatives NMC5 and NMC6 are also investigated.

Chart 1

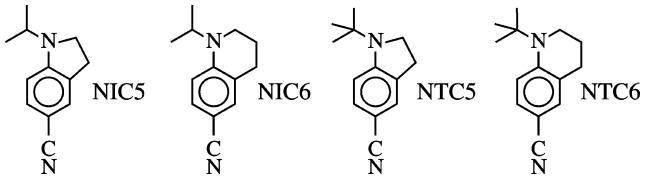

Chart 2

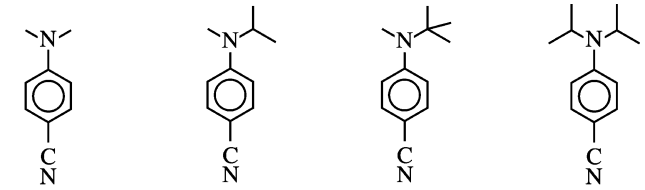

Experimental Section

To obtain NTC6, 1,2,3,4-tetrahydroquinoline in dimethylformamide was formylated with $POCl_3$, resulting in 3,4-dihydro-2*H*-quinoline-1-carbaldehyde (NCAC6).[33] NCAC6 was converted into 1,2,3,4-tetrahydroquinoline-6-carbaldehyde with $POCl_3$.[34] This compound was reacted with hydroxylamine hydrochloride in 1-methylpyrrolidone, giving 1,2,3,4-tetrahydroquinoline-6-carbonitrile (NHC6).[35] NHC6 in tetrahydrofuran (THF) was added slowly to a suspension consisting of CuI and *tert*-butyllithium in THF at −60 °C, followed by insertion of oxygen.[36] The product NTC6 was purified by flash chromatography and HPLC, checked by mass spectra. The molecular structure was established by NOE experiments. NTC5 was synthesized in an analogous manner. The detailed synthesis procedures and the NMR data are available as Supporting Information. For all aminobenzonitriles, HPLC was the last purification step. In the case of NTC6, for example, a purity of better than 99.5% is achieved, as no contaminants were visible in the HPLC after separation.

The solvents *n*-hexane and isopentane (Merck, Uvasol) were used as received. The other solvents were chromatographed over Al_2O_3. The solutions, with an optical density between 0.4 and 0.6 for the maximum of the first band in the absorption spectrum, were deaerated with nitrogen (15 min). The fluorescence spectra were measured with quantum-corrected Shimadzu RF-5000PC or ISA-SPEX Fluorolog 3-22 spectrofluorometers. Fluorescence quantum yields Φ_f, with an estimated reproducibility of 2%, were determined with quinine sulfate in 1.0 N H_2SO_4 as a standard ($\Phi_f = 0.546$ at 25 °C).[37]

The fluorescence decay times were determined with a picosecond laser system (excitation wavelength λ_{exc}: 276 nm) or a nanosecond (λ_{exc}: 296 nm) flashlamp single-photon counting (SPC) setup.[11,21,29] The instrument response function of the laser SPC system has a half-width of 18−20 ps, with an estimated time resolution of 3 ps.[29,30,32]

Results and Discussion

Absorption and Fluorescence Spectra of 4-Aminobenzonitriles in *n*-Hexane at 25 °C. Influence on ICT and $\Delta E(S_1,S_2)$ by Replacing Amino Methyl Groups with Isopropyl or *tert*-Butyl Substituents. The replacement of both amino methyl substituents in DMABN (Chart 2) by isopropyl groups results in the appearance of efficient intramolecular charge

(19) Jamorski Jödicke, C.; Lüthi, H. P. *J. Chem. Phys.* **2002**, *117*, 4146.
(20) Lommatzsch, U.; Brutschy, B. *Chem. Phys.* **1998**, *234*, 35.
(21) Leinhos, U.; Kühnle, W.; Zachariasse, K. A. *J. Phys. Chem.* **1991**, *95*, 2013.
(22) Günter, W.; Rettig, W. *J. Phys. Chem.* **1984**, *88*, 2729.
(23) Visser, R. J.; Varma, C. A. G. O. *J. Chem. Soc., Faraday Trans. 2* **1980**, *76*, 453.
(24) Rotkiewicz, K.; Grabowski, Z. R.; Krówczyński, A.; Kühnle, W. *J. Lumin.* **1976**, *12/13*, 877.
(25) Baumann, W.; Bischof, H.; Brittinger, J.-C.; Rettig, W.; Rotkiewicz, K. *J. Photochem. Photobiol., A: Chem.* **1992**, *64*, 49.
(26) Grabowski, Z. R. *Acta Phys. Pol.* **1987**, *A71*, 743.
(27) Zachariasse, K. A.; von der Haar, Th.; Hebecker, A.; Leinhos, U.; Kühnle, W. *Pure Appl. Chem.* **1993**, *65*, 1745.
(28) Zachariasse, K. A.; Grobys, M.; Tauer, E. *Chem. Phys. Lett.* **1997**, *274*, 372.
(29) Zachariasse, K. A.; Yoshihara, T.; Druzhinin, S. I. *J. Phys. Chem. A* **2002**, *106*, 6325. Erratum: *J. Phys. Chem. A* **2002**, *106*, 8978.
(30) Demeter, A.; Druzhinin, S.; George, M.; Haselbach, E.; Roulin, J.-L.; Zachariasse, K. A. *Chem. Phys. Lett.* **2000**, *323*, 351.
(31) Daum, R.; Druzhinin, S. I.; Ernst, D.; Rupp, L.; Schroeder, J.; Zachariasse, K. A. *Chem. Phys. Lett.* **2001**, *341*, 272.
(32) Druzhinin, S. I.; Demeter, A.; Zachariasse, K. A. *Chem. Phys. Lett.* **2001**, *347*, 421.
(33) Lukevits, É.; Zablotskaya, A.; Segal, I. *Chem. Heterocycl. Compd.* **1995**, *31*, 374.
(34) Gawinecki, R.; Sylwia, A.; Puchala, A. *Org. Prep. Proced. Int.* **1998**, *30*, 455. Private communication: Prof. R. Gawinecki.
(35) Sampath Kumar, H. M.; Subba Reddy, B. V.; Tirupathi Reddy, P.; Yadav, J. S. *Synthesis-Stuttgart* **1999**, 586.
(36) Yamamoto, H.; Maruoka, K. *J. Org. Chem.* **1980**, *45*, 2739.
(37) Demas, J. N.; Crosby, G. A. *J. Phys. Chem.* **1971**, *75*, 991.

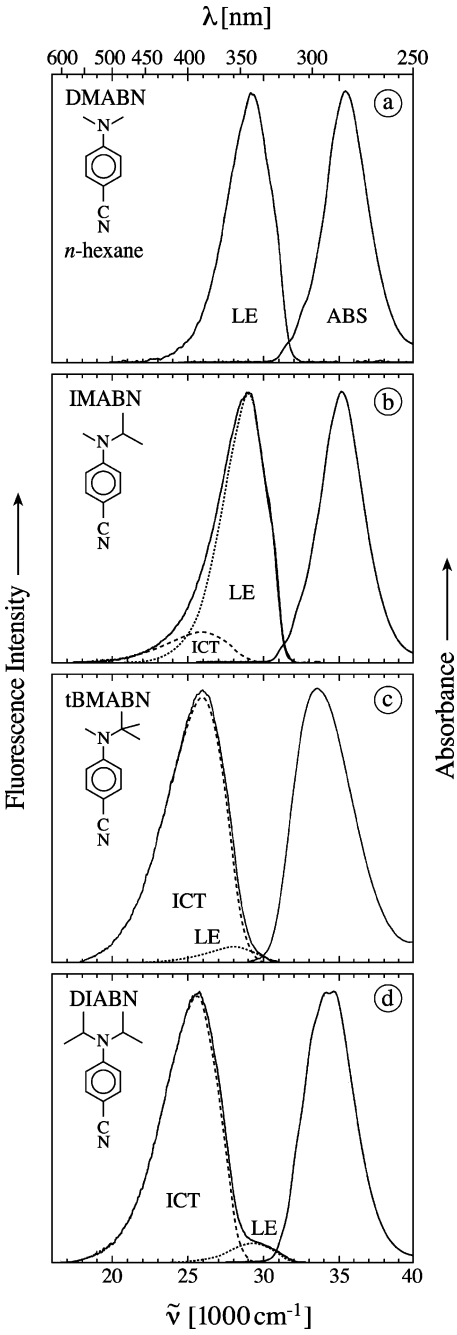

Figure 1. Fluorescence and absorption spectra in *n*-hexane at 25 °C of (a) 4-(dimethylamino)benzonitrile (DMABN), (b) 4-(isopropylmethylamino)-benzonitrile (IMABN), (c) 4-(*tert*-butylmethylamino)benzonitrile (tBMABN), and (d) 4-(diisopropylamino)benzonitrile (DIABN). The fluorescence spectrum of DMABN consists of a single LE emission, whereas IMABN, tBMABN, and DIABN are dual fluorescent (LE and ICT). Excitation in the maximum of the absorption spectra.

transfer (ICT) for DIABN in *n*-hexane, in contrast to DMABN, for which only an emission from a locally excited (LE) state is observed in this solvent,[30] see Figure 1a and 1d.

This difference has been attributed to the considerable decrease in the energy gap $\Delta E(S_1,S_2)$ between the S_1 and S_2 states of DIABN as compared with DMABN, as seen by inspecting the absorption spectra in Figure 1a and 1d.[30]

When only one methyl group of DMABN is replaced by isopropyl, giving 4-(isopropylmethylamino)benzonitrile (IMABN), a much smaller reduction of $\Delta E(S_1,S_2)$ is observed (Figure 1b) than for DIABN and the fluorescence spectrum mainly consists of an LE emission band, with a relatively small value of ~0.2 for $\Phi'(\mathrm{ICT})/\Phi(\mathrm{LE})$. Introduction of a *tert*-butyl group instead of isopropyl, however, results for 4-(*tert*-butylmethylamino)-benzonitrile (tBMABN) in a much larger reduction of the $\Delta E(S_1,S_2)$ energy gap as compared with DMABN and IMABN, see Figure 1c. For tBMABN in *n*-hexane, the absorption spectrum is similar to that of DIABN (Figure 1d), and the fluorescence spectrum likewise predominantly consists of an ICT emission band (Figure 1c).

The results presented in Figure 1 show empirically that the replacement of one of the methyl groups in DMABN by *tert*-butyl leads to a substantial decrease of the $\Delta E(S_1,S_2)$ energy gap and the appearance of efficient ICT in *n*-hexane at 25 °C, similar to what is observed when both methyl groups of DMABN are replaced by isopropyl in the case of DIABN. This is in clear contrast to what results from replacing a methyl group by isopropyl, which in IMABN only leads to a minor reduction of $\Delta E(S_1,S_2)$ and the appearance of a small amount of ICT fluorescence. This pronounced influence of the introduction of a *tert*-butyl substituent as compared with isopropyl on the enhancement of ICT was the basis for the investigations presented in this paper for two series of planarized aminobenzonitriles, the 1-alkyl-6-cyano-1,2,3,4-tetrahydroquinolines NXC6 (NMC6, NIC6, NTC6) and the 1-alkyl-5-cyanoindolines NXC5 (NMC5, NIC5, NTC5) with methyl (M), isopropyl (I), and *tert*-butyl (T) alkyl substituents.

Absorption Spectra of NXC6 and NXC5 in *n*-Hexane and Acetonitrile at 25 °C. The absorption spectra of the 1-alkyl-6-cyano-1,2,3,4-tetrahydroquinolines NMC6, NIC6, NTC6 and the 1-alkyl-5-cyanoindolines NMC5, NIC5, and NTC5 in *n*-hexane and acetonitrile at 25 °C are shown in Figure 2. The molar extinction coefficients $\epsilon^{\max}$ measured at the maxima of the main absorption bands of NMC5, NEC5, NIC5, NMC6, NEC6, NIC6, and NTC6 in *n*-hexane all have a value around 22 000 $\mathrm{M^{-1}\,cm^{-1}}$ (Table 1), which means that the structure of the amino group is similar in these compounds. This is based on the observation that for 4-aminobenzonitriles the amino twist angle θ in the ground state determines $\epsilon^{\max}$ according to the relation $\epsilon^{\max}$ is proportional to $\cos^2\theta$.[38,39]

In the case of NMC6 and NIC6 in *n*-hexane, the absorption spectrum is similar to that of DMABN (Figure 1a) with well-separated S_1 and S_2 bands. Replacing the isopropyl substituent of NIC6 by a *tert*-butyl group (NTC6) leads, however, to a reduction of the $\Delta E(S_1,S_2)$ energy gap caused by a red-shift of the S_2 band, with a difference between the absorption spectra of NTC6 and NIC6 comparable to that found for the pair DIABN/DMABN, see Figure 1. For the three indolines NMC5, NIC5, and NTC5 in *n*-hexane, an influence of the 1-alkyl substituent on $\Delta E(S_1,S_2)$ is found to be similar to that for the three corresponding tetrahydroquinolines. The comparison of the spectra of NTC6 and NTC5 reveals that the S_1 band becomes more visible in the indoline derivative, indicating that the reduction of the size of the alicyclic ring leads to an overall increase in the $\Delta E(S_1,S_2)$ energy gap. The absorption spectra of NXC6 and NXC5 in acetonitrile (Figure 2, dashed lines) do not reveal a clearly separated S_1 band, due to the preferential red-shift of the main S_2 absorption band.

(38) Burgers, J.; Hoefnagel, M. A.; Verkade, P. E.; Visser, H.; Wepster, B. M. *Recl. Trav. Chim. Pays-Bas* **1958**, *77*, 491.
(39) Rückert, I.; Hebecker, A.; Parusel, A. B. J.; Zachariasse, K. A. *Z. Phys. Chem.* **2000**, *214*, 1597.

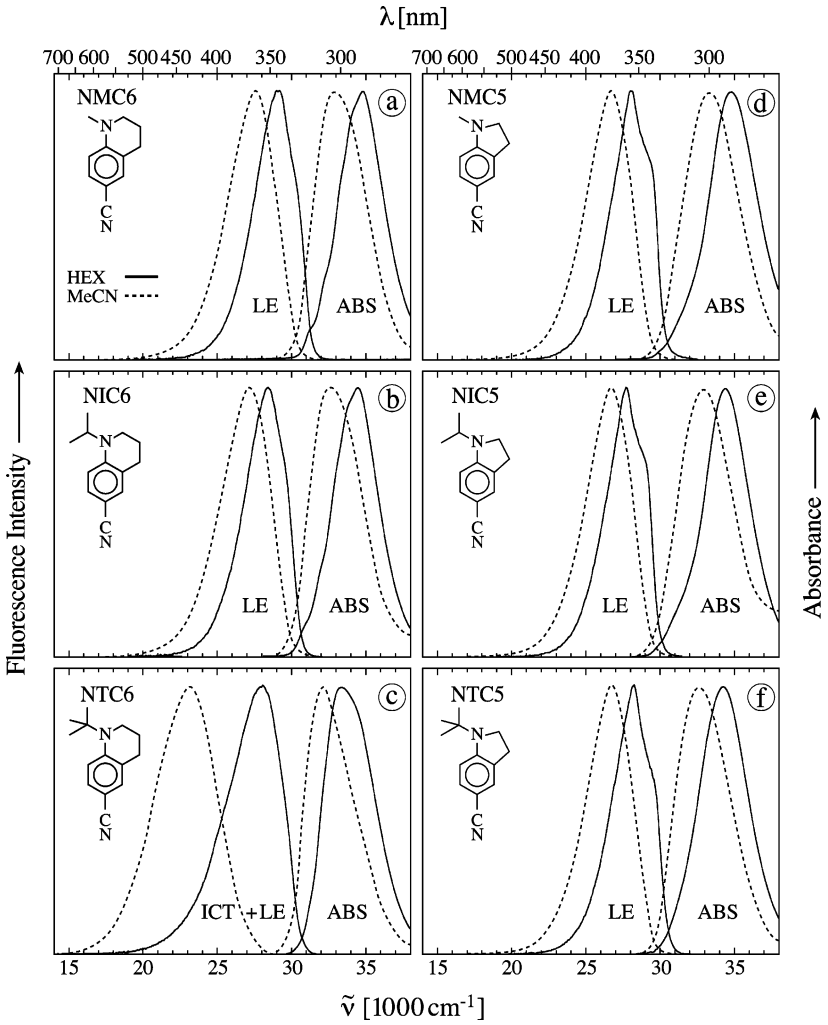

Figure 2. Fluorescence and absorption spectra at 25 °C in *n*-hexane (HEX, solid line) and acetonitrile (MeCN, dashed line) of (a) 1-methyl-6-cyano-1,2,3,4-tetrahydroquinoline (NMC6), (b) 1-isopropyl-6-cyano-1,2,3,4-tetrahydroquinoline (NIC6), (c) 1-*tert*-butyl-6-cyano-1,2,3,4-tetrahydroquinoline (NTC6), (d) 1-methyl-5-cyanoindoline (NMC5), (e) 1-isopropyl-5-cyanoindoline (NIC5), and (f) 1-*tert*-butyl-5-cyanoindoline (NTC5). The fluorescence spectrum of all molecules except NTC6 consists of a single LE emission in both solvents, whereas NTC6 is dual fluorescent (LE and ICT) in *n*-hexane as well as in acetonitrile. Excitation in the maximum of the absorption spectra (not shown).

Table 1. Extinction Coefficients ϵ^{max} Measured at the Maximum λ^{max} of the Main Absorption Band of Compounds NXC5 and NXC6 in *n*-Hexane at 25 °C, See Figure 2

	NMC5	NEC5	NIC5	NMC6	NEC6	NIC6	NTC6
ϵ^{max} [M^{-1} cm^{-1}]	21 120	21 200	23 660	21 800	22 840	22 970	21 310
λ^{max} [nm]	287.7	289.6	291.0	287.2	289.2	290.0	298.8

Fluorescence Spectra of NXC6 and NXC5 in *n*-Hexane and Acetonitrile at 25 °C. The fluorescence spectra of NXC6 and NXC5 in *n*-hexane and acetonitrile are shown in Figure 2. The spectrum of NIC6 in *n*-hexane (Figure 2b) resembles that of NMC6 (Figure 2a) and DMABN (Figure 1a), which means that the replacement of the single methyl substituent at the amino nitrogen of NMC6 by isopropyl does not lead to dual fluorescence and ICT in *n*-hexane at 25 °C, contrary to what is found for the aminobenzonitriles in Figure 1. The introduction of a *tert*-butyl group (NTC6), however, does in fact result in a substantial broadening of the spectrum. This broadening and red-shift of the fluorescence spectrum of NTC6 as compared with that of NIC6 and NMC6 has become clearly larger in the polar solvent acetonitrile (Figure 2c). The emission band of NTC6 is strongly red-shifted as compared with NMC6 and NIC6, with a Stokes shift $\Delta\tilde{\nu}^{max}(ST) = \tilde{\nu}^{max}(abs) - \tilde{\nu}^{max}(flu)$ between the maxima of the absorption and fluorescence spectra of 9000 cm^{-1}, considerably larger than $\Delta\tilde{\nu}^{max}(ST)$ for NIC6 (5400 cm^{-1}) and NMC6 (5300 cm^{-1}). These spectral results are interpreted as indications of the occurrence of an ICT reaction in the case of NTC6, the interpretation of which will be further elaborated in the following sections.

For the indolines NMC5, NIC5, and NTC5 in *n*-hexane and acetonitrile (Figure 2d−f), the fluorescence spectra consist of a single LE band, showing that when the size of the alicyclic ring is reduced from six to five, an ICT reaction does not occur upon replacing the isopropyl in NIC5 by a *tert*-butyl substituent (NTC5). This reduction in ring size leads to an increase of $\Delta E(S_1,S_2)$, see Figure 2, as discussed in the previous section.[12,13]

The Energy Gap $\Delta E(S_1,S_2)$ and Intramolecular Charge Transfer. The strong increase in the efficiency of the ICT reaction in *n*-hexane for DIABN as compared with that for

Table 2. Solvent Parameters and Fluorescence Maxima $\tilde{\nu}^{max}$ (in 1000 cm^{-1}) for NTC6, ICT of NTC6, and LE for NIC6, NMC6, NTC5, NIC5, NMC5

			NTC6		NIC6	NMC6	NTC5	NIC5	NMC5
solvent	$f(\epsilon) - f(n^2)$[a]	$f(\epsilon) - {}^1/_2 f(n^2)$[a]	LE + ICT	ICT	LE	LE	LE	LE	LE
n-hexane (1)	0	0.092	28.21	(26.55)	28.56	29.06	28.17	28.20	28.06
cyclopentane (2)	−0.001	0.097	28.00	(26.63)	28.52				
n-hexadecane (3)	−0.001	0.102	28.07	(26.70)	28.53				
cis-decaline (4)	0.002	0.113	27.87	(26.69)	28.40				
di(*n*-hexyl) ether (5)	0.067	0.168	27.09	26.89	28.26				
di(*n*-pentyl) ether (6)	0.077	0.177	26.97	26.86	28.25		27.88	27.57	
di(*n*-butyl) ether (7)	0.095	0.192	26.86	26.70	28.22	28.61	27.90	27.56	27.68
di(*n*-propyl) ether (8)	0.113	0.207	26.67	26.52	28.20		27.86	27.55	
diethyl ether (9)	0.165	0.253	26.10	26.05	28.07	28.40	27.66	27.39	27.41
n-butyl acetate (10)	0.170	0.266	25.20	25.04	27.73				
n-propyl acetate (11)	0.187	0.281	25.01	24.87	27.71				
ethyl acetate (12)	0.200	0.292	24.73	24.66	27.65	27.94	27.28	27.05	27.05
methyl acetate (13)	0.218	0.308	24.34	24.34	27.59				
tetrahydrofuran (14)	0.208	0.307	24.90	24.80	27.65	27.99	27.30	27.05	27.01
dichloromethane (15)	0.218	0.319	24.19	24.19	27.54				
1,2-dichloroethane (16)	0.221	0.326	24.08	24.08	27.53	27.99	27.21	26.99	27.06
n-butyl cyanide (17))	0.269	0.366	23.85	23.85	27.39				
n-propyl cyanide (18)	0.281	0.375	23.75	23.75	27.37				
ethyl cyanide (19)	0.293	0.383	23.53	23.53	27.29		27.01		
acetonitrile (20)	0.306	0.393	23.13	23.13	27.24	27.56	26.75	26.49	26.66
methanol (21)	0.309	0.393	22.60	22.60	27.21				

[a] $f(\epsilon) = (\epsilon - 1)/(2\epsilon + 1)$, $f(n^2) = (n^2 - 1)/(2n^2 + 1)$.

DMABN has been attributed to the decrease of the energy gap $\Delta E(S_1,S_2)$, which leads to a lowering of the energy of the ICT state relative to the equilibrated LE(S_1) state, as outlined above.[12,13,30] Inspection of the fluorescence and absorption spectra in Figure 2 shows that a similar situation holds for the pairs NTC6/NIC6 and NTC6/NTC5. It is therefore concluded that the reduction of $\Delta E(S_1,S_2)$ caused by the replacement of methyl by isopropyl (DMABN/DIABN) as well as that of isopropyl by *tert*-butyl (NIC6/NTC6) is the reason for the strong enhancement of the ICT efficiency in the case of DIABN and NTC6. A similar effect on $\Delta E(S_1,S_2)$ is brought about by the increase of the alicyclic ring size from five (NTC5) to six (NTC6).

Fluorescence Spectra of NXC6 and NXC5 as a Function of Solvent Polarity at 25 °C. The fluorescence spectra of the three tetrahydroquinolines NXC6 and the three indolines NXC5 (X = M, I, T) were measured at 25 °C in a series of solvents with increasing polarity, from *n*-hexane to acetonitrile and methanol, see Table 2. The red-shift of the spectra, gradually becoming larger with increasing solvent polarity, is much larger for NTC6 than for NIC6 and NMC6 and NXC5 (Table 2 and Figure 2). These findings support our interpretation that of the NXC6 and NXC5 compounds only NTC6 undergoes ICT. At first sight, there is, however, no direct spectral indication for two separate emission bands (dual fluorescence) in the spectra of NTC6. By a solvatochromic analysis of the maxima of the fluorescence bands,[40] the excited-state dipole moment can be determined, from which the ICT or LE character of an emission spectrum can be decided. This analysis is presented for NXC6 and NXC5 in the next section.

Solvatochromic Measurements. Excited-State Dipole Moments μ_e(LE) and μ_e(ICT) of NXC6 and NXC5 at 25 °C. To determine the excited-state dipole moment μ_e of the molecules NXC6 and NXC5, the energies $\tilde{\nu}^{max}$(flu) of the maxima of their emission bands are plotted against the polarity parameter $f(\epsilon,n)$, see eqs 1−3, where ϵ is the dielectric constant, n is the refractive index, and ρ is the Onsager radius of the solute.[25,41,42] For an LE state, the applicable polarity function $f(\epsilon,n)$ is $f(\epsilon) - f(n^2)$, whereas $f(\epsilon,n) = f(\epsilon) - {}^1/_2 f(n^2)$ is used for an ICT state.[41−45]

$$\tilde{\nu}^{max}(\text{flu}) = -\frac{1}{2hc\rho^3}\mu_e(\mu_e - \mu_g)f(\epsilon,n) + \text{const.} \qquad (1)$$

$$f(\epsilon) = \frac{(\epsilon - 1)}{(2\epsilon + 1)} \qquad (2)$$

$$f(n^2) = \frac{(n^2 - 1)}{(2n^2 + 1)} \qquad (3)$$

Solvatochromic Plots for NIC6 and NTC6. The maxima $\tilde{\nu}^{max}$(flu) of the fluorescence bands of NIC6 and NTC6 (Table 2) are plotted in Figure 3 against the solvent polarity parameter $f(\epsilon) - {}^1/_2 f(n^2)$. It is seen that the solvent polarity dependence of $\tilde{\nu}^{max}$(flu) is much more pronounced for NTC6 than for NIC6. The maxima of NIC6 undergo a red-shift of 1350 cm^{-1} with increasing solvent polarity from *n*-hexane (28 560 cm^{-1}) to methanol (27 210 cm^{-1}). For NTC6, a much larger red-shift (5610 cm^{-1}) is observed, from 28 210 cm^{-1} in *n*-hexane to 22 600 cm^{-1} in methanol. For NMC6 and the three NXC5 molecules, only a relatively small red-shift of $\tilde{\nu}^{max}$(flu) with increasing solvent polarity is found (Table 2), similar to that obtained with NIC6.

Nonlinear Solvatochromic Plot for NTC6. Dual Fluorescence. Whereas a single straight line can be used to fit the data points for NIC6 in Figure 3a, two straight lines with different

(40) Suppan, P.; Ghoneim, N. *Solvatochromism*; The Royal Society of Chemistry: Cambridge, UK, 1997; Chapter 7.

(41) Liptay, W. In *Excited states*; Lim, E. C., Ed.; Academic Press: New York, 1974; Vol. 1, p 129.

(42) Il'ichev, Yu. V.; Kühnle, W.; Zachariasse, K. A. *Chem. Phys.* **1996**, *211*, 441.

(43) Schuddeboom, W.; Jonker, S. A.; Warman, J. M.; Leinhos, U.; Kühnle, W.; Zachariasse, K. A. *J. Phys. Chem.* **1992**, *96*, 10809.

(44) Yoshihara, T.; Galievsky, V.; Druzhinin, S. I.; Saha, S.; Zachariasse, K. A. *Photochem. Photobiol. Sci.* **2003**, *2*, 342.

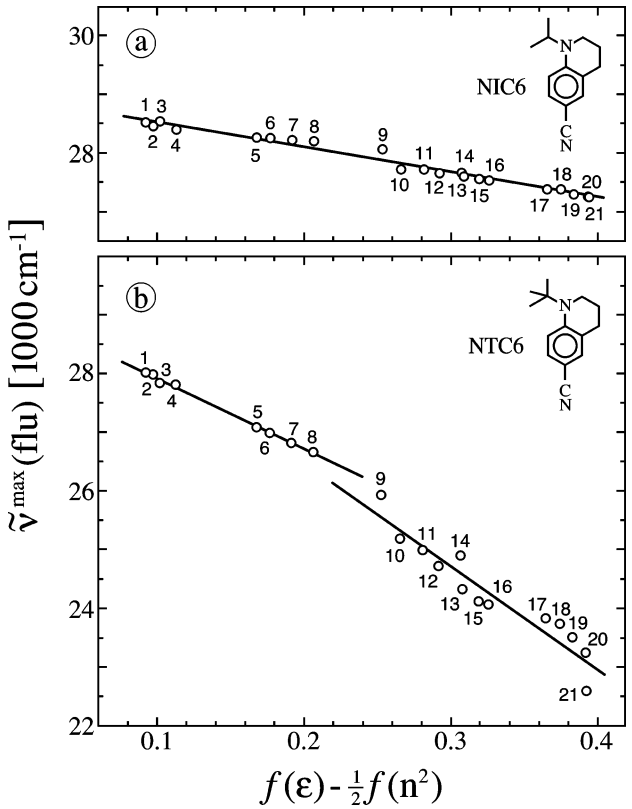

Figure 3. Fluorescence emission maxima $\tilde{\nu}^{max}$(flu) of (a) 1-isopropyl-6-cyano-1,2,3,4-tetrahydroquinoline (NIC6) and (b) 1-*tert*-butyl-6-cyano-1,2,3,4-tetrahydroquinoline (NTC6) at 25 °C against the solvent polarity parameter $f(\epsilon) - {}^1/_2 f(n^2)$, see eqs 1−3. The numbers refer to the solvents in Table 2.

slopes are necessary to fit the data in the case of NTC6, see Figure 3b. This nonlinear polarity dependence of $\tilde{\nu}^{max}$(flu) shows that the fluorescence spectrum of NTC6 consists of two bands. The difference in polar character of the excited states responsible for the fluorescence bands of NIC6 and NTC6 can be established by determining their dipole moments, as will be discussed in subsequent sections. The observation of a nonlinear solvatochromic plot for NTC6 is in accord with the conclusion presented in the previous sections that ICT takes place with NTC6, but not with NIC6, NMC6, and NXC5 molecules. Nonlinear solvatochromic plots have been observed before, such as with 6-cyanobenzoquinuclidine (CBQ)[46] and the 6-(phenylamino)-2-naphthalenesulfonate (6,2-ANS),[47] interpreted in the case of 6,2-ANS as originating from the presence of emission bands from two excited states with different charge distributions.

LE Dipole Moments μ_e(LE) of NIC6, NMC6, and NXC5. From the much smaller solvent polarity dependence of NIC6 as compared with NTC6 (Figure 3), it can already be concluded that the excited state of NIC6 will have a relatively small dipole moment and hence will be an LE state. Its dipole moment μ_e(LE) is determined by plotting $\tilde{\nu}^{max}$(flu) against $f(\epsilon) - f(n^2)$, see eqs 1−3. The same procedure is followed for NMC6 and the three NXC5 compounds. The plots are presented in Figure 4. In all cases, a single straight line adequately fits the data points. From the slope of these plots (Table 3), the following

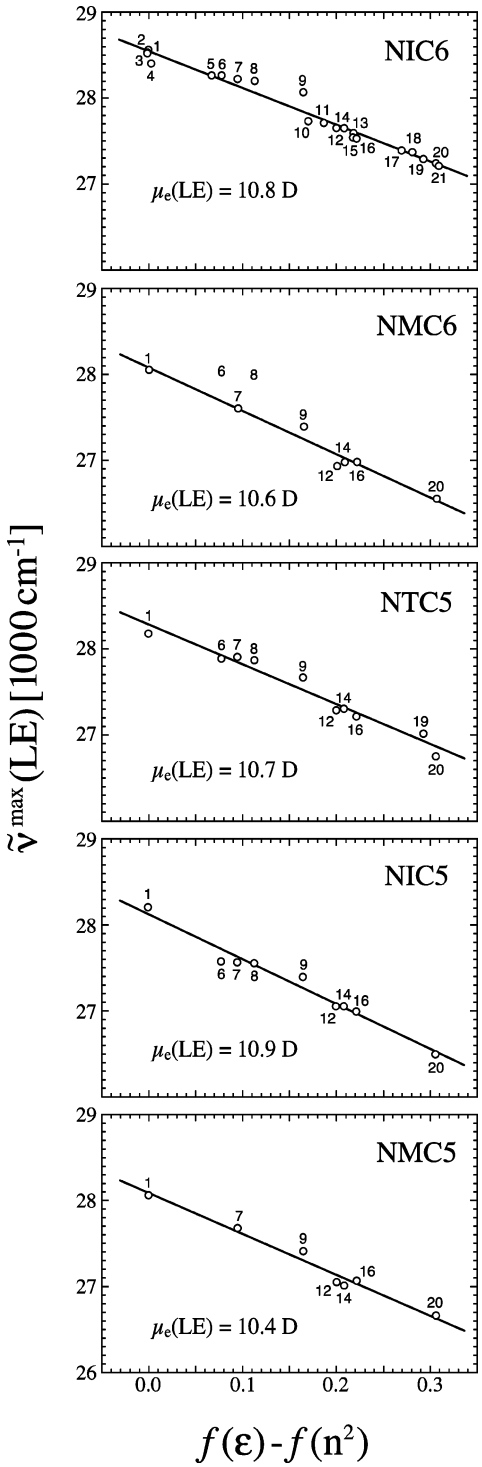

Figure 4. LE fluorescence emission maxima $\tilde{\nu}^{max}$(LE) of 1-isopropyl-6-cyano-1,2,3,4-tetrahydroquinoline (NIC6), 1-methyl-6-cyano-1,2,3,4-tetrahydroquinoline (NMC6), 1-*tert*-butyl-5-cyanoindoline (NTC5), 1-isopropyl-5-cyanoindoline (NIC5), and 1-methyl-5-cyanoindoline (NMC5) in a series of solvents at 25 °C against the solvent polarity parameter $f(\epsilon) - f(n^2)$, see eqs 1−3. The numbers refer to the solvents in Table 2.

dipole moments μ_e(LE) are determined: 10.8 ± 0.1 D (NIC6), 10.6 ± 0.2 D (NMC6), 10.7 ± 0.2 D (NTC5), 10.9 ± 0.2 D (NIC5), and 10.4 ± 0.2 D (NMC5). These values are similar to that for μ_e(LE) of DMABN (10 D),[43,44] indicating that the excited state of NIC6, NMC6, and NXC5 indeed has the character of an LE state, meaning that ICT does not take place with these molecules.

(45) Beens, H.; Weller, A. *Acta Phys. Pol.* **1968**, *34*, 593.
(46) Köhler, G.; Rechthaler, K.; Grabner, G.; Luboradzki, R.; Suwińska, K.; Rotkiewicz, K. *J. Phys. Chem. A* **1997**, *101*, 8518.
(47) Dodiuk, H.; Kosower, E. M. *J. Am. Chem. Soc.* **1977**, *99*, 859.

Table 3. Dipole Moments for the Ground State (μ_g), for the ICT State of NTC6, and for the LE State of NIC6, NMC6, NTC5, NIC5, and NMC5 (μ_e), Derived from Solvatochromic Measurements, See Eqs 1−3

substance (model)	band (model)	ρ [Å]	μ_g [D]	$\Delta\tilde{\nu}^{max}/\Delta f(\epsilon,n)$ [1000 cm^{-1}]	$\Delta\tilde{\nu}^{max}$(NTC6)/ $\Delta\tilde{\nu}^{max}$(model)	μ_e (μ_g) of model [D]	μ_e [D]
NTC6	ICT	4.78	6.80	−17.47 ± 0.91			17.6 ± 0.4
NTC6	total[a]	4.78	6.80	−18.01 ± 1.82			17.8 ± 0.7
NTC6	total[b]	4.78	6.80	−16.75 ± 0.53			17.3 ± 0.2
NTC6 (DIABN)	ICT (ICT)		6.80		0.945 ± 0.018	19.2 (6.78)	19.2 ± 0.2
NTC6 (DMABN)	ICT (ICT)		6.80		0.881 ± 0.023	17 (6.6)	18.9 ± 0.2
NTC6 (PP4C)	ICT (ICT)		6.80		0.614 ± 0.016	18.3 (3.18)	18.5 ± 0.2
NTC6 (PP3C)	ICT (ICT)		6.80		0.607 ± 0.015	17.4 (3.56)	17.5 ± 0.2
NTC6 (NIC6)	ICT (LE)		6.80		3.52 ± 0.007	10.9 (6.80)	16.8 ± 0.1
NIC6	LE	4.67	6.80	−4.27 ± 0.16			10.8 ± 0.1
NMC6	LE	4.32	6.80	−5.02 ± 0.38			10.6 ± 0.2
NTC5	LE	4.67	6.39	−4.61 ± 0.33			10.7 ± 0.2
NIC5	LE	4.56	6.39	−5.21 ± 0.33			10.9 ± 0.2
NMC5	LE	4.44	6.39	−4.75 ± 0.32			10.4 ± 0.2

[a] Total band, not subtracted, in polar solvents 9−20, see Table 2, mainly ICT emission. [b] Total band, not subtracted, in solvents 1−20, see Table 2.

Table 4. Fluorescence Quantum Yields Φ(LE) of NMC6, NIC6, NMC5, NIC5, and NTC5 at 25 °C

solvent	NMC6	NIC6	NMC5	NIC5	NTC5
n-hexane (1)	0.244	0.188			
diethyl ether (9)	0.228	0.191	0.237	0.233	0.236
tetrahydrofuran (14)		0.205			
n-propyl cyanide (18)		0.223			
acetonitrile (20)	0.229	0.230	0.196	0.229	0.202

Table 5. Fluorescence Quantum Yields and ICT/LE Quantum Yield Ratios Φ′(ICT)/Φ(LE) of NTC6 at 25 °C

solvent	Φ(total)	Φ′(ICT)	Φ(LE)	Φ′(ICT)/Φ(LE)
n-hexane (1)	0.22	0.086	0.134	0.64
cyclopentane (2)				0.79
n-hexadecane (3)	0.22	0.105	0.115	0.91
cis-decaline (4)				0.87
di(*n*-hexyl) ether (5)				2.3
di(*n*-pentyl) ether (6)	0.43	0.317	0.113	2.8
di(*n*-butyl) ether (7)	0.39	0.290	0.100	2.9
di(*n*-propyl) ether (8)				3.6
diethyl ether (9)	0.51	0.445	0.065	6.8
n-butyl acetate (10)				14
n-propyl acetate (11)				16
ethyl acetate (12)	0.58	0.552	0.028	20
methyl acetate (13)				27
tetrahydrofuran (14)	0.58	0.548	0.032	17
toluene (23)	0.43			
dichloromethane (15)				52
1,2-dichloroethane (16)				50
n-butyl cyanide (17)				43
n-propyl cyanide (18)	0.58	0.570	0.010	57
ethyl cyanide (19)	0.55	0.542	0.075	72
acetonitrile (20)	0.54	0.536	0.004	121
methanol (21)				192

In accordance with this conclusion, the fluorescence quantum yields of NMC6, NIC6, and the three NXC5 molecules do not strongly depend on solvent polarity when going from *n*-hexane or diethyl ether to acetonitrile, see Table 4, in contrast to what is observed with dual fluorescent molecules such as DMABN.[8,9,28]

Spectral Subtraction of Overlapping LE and ICT Bands of NTC6 and Dipole Moment μ_e(ICT). From the slope of the line for the solvents diethyl ether to acetonitrile in the solvatochromic plot for NTC6 (Figure 3b and eq 1), a dipole moment μ_e of 17.8 ± 0.7 D is obtained (Table 3). On the basis of this value of 18 D and the nonlinear character of the solvatochromic plot of NTC6, it is therefore concluded that the fluorescence spectra of NTC6 consist of contributions from an LE and an ICT state. These LE and ICT emissions can be separated by spectral subtraction with NIC6 as the model compound, as shown in Figure 5. This molecule only differs from NTC6 in the N-alkyl substituent, and its emission spectrum consists of a single LE band (Figures 2 and 4). It is seen from Table 5 that the relative contribution of ICT fluorescence to the total emission spectrum, the ICT/LE fluorescence quantum yield ratio Φ′(ICT)/Φ(LE), of NTC6 at 25 °C increases when the solvent polarity becomes larger, from 0.64 in *n*-hexane, via 17 in tetrahydrofuran, to 121 in acetonitrile and 192 in methanol.

The data for $\tilde{\nu}^{max}$(ICT) of the separated ICT band of NTC6 in the solvents *n*-hexane to tetrahydrofuran are listed in Table 2. For the other solvents, $\tilde{\nu}^{max}$(ICT) does not differ from $\tilde{\nu}^{max}$(flu) (Table 2). From a solvatochromic plot of these data for $\tilde{\nu}^{max}$(ICT) against $f(\epsilon) - {}^1/_2 f(n^2)$ in Figure 6, a dipole moment μ_e(ICT) of 17.6 ± 0.4 D is determined, see Table 3.

The increase in the slope of the solvatochromic plot for NTC6 for solvents more polar than diethyl ether as compared with the less polar solvents (Figure 3b) hence means that for the more polar solvents, the major contribution to the overall fluorescence spectrum comes from the ICT state. For the solvents between *n*-hexane and diethyl ether, however, the data points are the maxima of composite LE and ICT bands. It is then clear that the presence of the LE emission band with a smaller solvatochromic slope $\mu_e(\mu_e - \mu_g)$ (eq 1) reduces the effective slope of this plot. For this reason, the solvatochromic analysis to determine μ_e(ICT) of NTC6 in the previous section was limited to the solvents diethyl ether to acetonitrile.

ICT Dipole Moment μ_e(ICT) of NTC6 Relative to DIABN, DMABN, PP4C, and PP3C. The ICT dipole moment of NTC6 can also be obtained from a plot of $\tilde{\nu}^{max}$(ICT) against the ICT maxima of a model compound such as DIABN, DMABN, *N*-(4-cyanophenyl)pyrrole (PP4C), or *N*-(3-cyanophenyl)pyrrole (PP3C),[30,44] see Figure 7, Table 6, and ref 44 for PP3C. By employing this procedure, the scatter in the data points as appearing in Figure 3b, generally observed when plotting $\tilde{\nu}^{max}$(ICT) against the solvent polarity parameter $f(\epsilon) - {}^1/_2 f(n^2)$,[25,30,42,44] is reduced by mutually compensating the specific solute/solvent interactions.[30]

The slope of the plot in Figure 7a is equal to the expression $\mu_e(\mathrm{ICT})(\mu_e(\mathrm{ICT}) - \mu_g(\mathrm{FC}))/\rho^3$ (see eq 1) for NTC6 divided by that for DMABN. From this slope (0.88 ± 0.02), an ICT dipole moment μ_e(ICT) of 18.9 ± 0.2 D is calculated for NTC6 (Table 3), based on the dipole moment of 17 D for the ICT state of

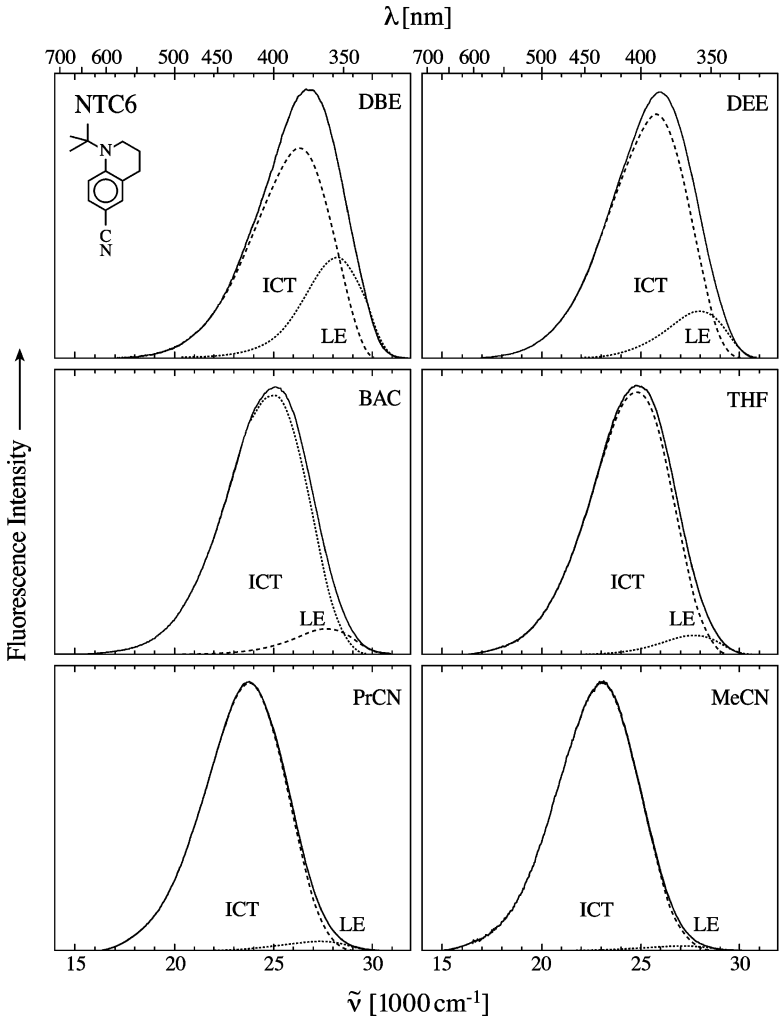

Figure 5. Fluorescence spectra of 1-*tert*-butyl-6-cyano-1,2,3,4-tetrahydroquinoline (NTC6) at 25 °C. HEX, *n*-hexane; DBE, di(*n*-butyl) ether; DEE, diethyl ether; THF, tetrahydrofuran; PrCN, *n*-propyl cyanide; MeCN, acetonitrile. The separate emissions from the LE and ICT states are shown. In the spectral subtraction, 1-isopropyl-6-cyano-1,2,3,4-tetrahydroquinoline (NIC6) is used as a model compound for the LE state.

DMABN,[43] which has been determined by the TRMC method. From the $\tilde{\nu}^{max}$(ICT) plot of NTC6 versus DIABN (Figure 7b), a value of 19.2 ± 0.2 D results for μ_e(ICT) of NTC6. Similar values are obtained from plots of the $\tilde{\nu}^{max}$(ICT) data of NTC6 against those of PP4C and PP3C, see Table 3. In this method (see Figure 7), the impact of the Onsager radius ρ (eq 1) obviously is much smaller than when the ratio $\mu_e(ICT)(\mu_e(ICT) - \mu_g)/\rho^3$ is used directly in the dipole moment determination (Figures 3b and 6).

The value of 19 D for μ_e(ICT) of NTC6 indicates that the strongly Stokes-shifted main fluorescence band of NTC6 in solvents more polar than diethyl ether indeed originates from an ICT state, with a similar dipole moment and hence intramolecular charge separation as that observed with the not-planarized molecules DIABN, DMABN, and PP4C.

Fluorescence Quantum Yield Ratio Φ′(ICT)/Φ(LE) of NTC6 in Dibutyl Ether as a Function of Temperature. The fluorescence spectra of NTC6 in a number of solvents were measured as a function of temperature. As an example, the ICT/LE fluorescence quantum yield ratio Φ′(ICT)/Φ(LE), see eq 4, was determined for NTC6 in di(*n*-butyl) ether (DBE) from 140 °C down to −90 °C (Figure 8). NIC6, only showing LE emission over the entire temperature range, was again used as

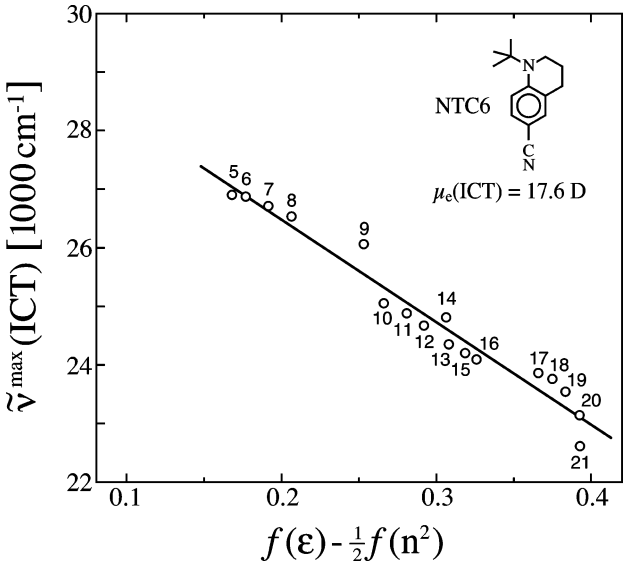

Figure 6. Fluorescence emission maxima $\tilde{\nu}^{max}$(ICT) of 1-*tert*-butyl-6-cyano-1,2,3,4-tetrahydroquinoline (NTC6) at 25 °C against the solvent polarity parameter $f(\epsilon) - {}^1/_2 f(n^2)$, see eqs 1−3. The numbers refer to the solvents in Table 2.

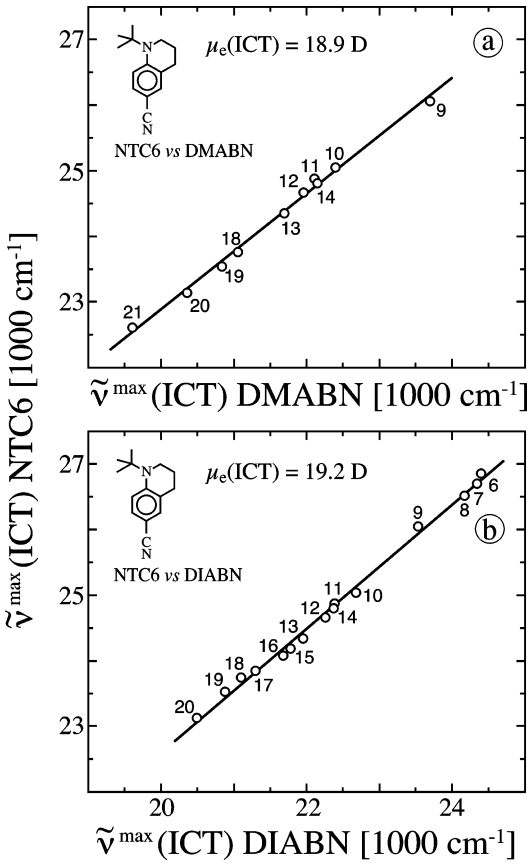

Figure 7. ICT fluorescence emission maxima $\tilde{\nu}^{max}$(ICT) of 1-*tert*-butyl-6-cyano-1,2,3,4-tetrahydroquinoline (NTC6) at 25 °C against the corresponding data of (a) 4-(dimethylamino)benzonitrile (DMABN) and (b) 4-(diisopropylamino)benzonitrile (DIABN), see eqs 1−3. The numbers refer to the solvents in Table 2.

Table 6. Solvent Parameters and Fluorescence Maxima $\tilde{\nu}^{max}$ (ICT) (in 1000 cm^{-1}) for DIABN, DMABN, and PP4C

solvent	$f(\epsilon) - {}^1/_2 f(n^2)$	DIABN	DMABN	PP4C
n-hexane (1)	0.092	25.73	*a*	29.30
n-hexadecane (3)	0.102	25.57	*a*	29.09
di(*n*-pentyl) ether (6)	0.177	24.40		26.83
di(*n*-butyl) ether (7)	0.192	24.34	(25.20)	26.64
di(*n*-propyl) ether (8)	0.207	24.17	(24.50)	26.24
diethyl ether (9)	0.253	23.53	23.70	25.17
n-butyl acetate (10)	0.266	22.68	22.40	23.49
n-propyl acetate (11)	0.281	22.38	22.11	23.26
ethyl acetate (12)	0.292	22.26	21.96	23.15
methyl acetate (13)	0.308	21.95	21.70	22.66
tetrahydrofuran (14)	0.307	22.37	22.15	23.30
dichloromethane (15)	0.319	21.78	22.77	23.40
1,2-dichloroethane (16)	0.326	21.68	22.44	23.05
n-butyl cyanide (17))	0.366	21.30	20.84	
n-propyl cyanide (18)	0.375	21.10	21.06	21.60
ethyl cyanide (19)	0.383	20.88	20.84	21.32
acetonitrile (20)	0.393	20.49	20.36	20.98
methanol (21)	0.393		19.61	

[a] No ICT emission.

the model compound for LE in the spectral subtraction procedure.

$$\Phi'(\mathrm{ICT})/\Phi(\mathrm{LE}) = k_f'/k_f \{k_a/(k_d + 1/\tau_o')\} \qquad (4)$$

In eq 4 and Scheme 1, k_a and k_d are the rate constants of the forward and backward ICT reaction, τ_o(LE) and τ_o'(ICT) are the fluorescence lifetimes, and k_f(LE) and k_f'(ICT) are the radiative rate constants.

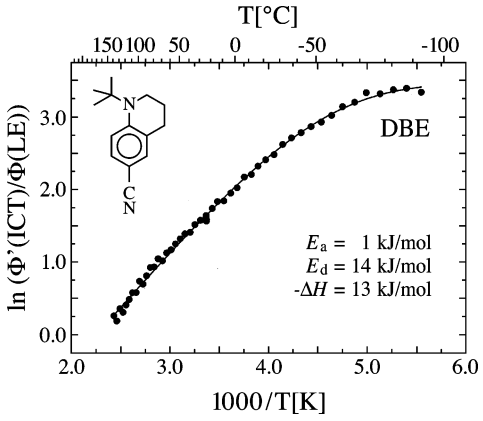

Figure 8. Plot of the natural logarithm of the LE/ICT fluorescence quantum yield ratio Φ'(ICT)/Φ(LE) versus the reciprocal absolute temperature for 1-*tert*-butyl-6-cyano-1,2,3,4-tetrahydroquinoline (NTC6) in di(*n*-butyl) ether (DBE). The activation energies of the LE → ICT (E_a) and ICT → LE (E_d) reactions and the enthalpy difference $-\Delta H$ between the LE and ICT states are indicated in the Figure, see Schemes 1 and 2. The line through the data points represents the fitting of the data with eq 4.

Scheme 1

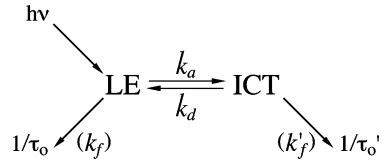

Scheme 2

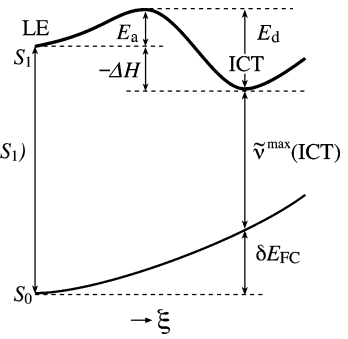

It is seen from the Stevens−Ban plot for NTC6 in DBE in Figure 8 that Φ'(ICT)/Φ(LE) becomes larger upon lowering the temperature, without reaching a maximum, where $k_d = 1/\tau_o'$.[21] This means that NTC6 in DBE is in the high-temperature limit (HTL), for which $k_d \gg 1/\tau_o'$.[48−50] In the case of DMABN, the HTL condition is encountered in solvents such as toluene. For this system with a relatively small $-\Delta H$ (8 kJ/mol), $k_d = 45 \times 10^9$ s^{-1} and $1/\tau_o' = 0.4 \times 10^9$ s^{-1} at 20 °C.[11,21]

The potential energy surfaces and energies describing the LE ⇌ ICT reaction are depicted in Scheme 2, where $E(S_1)$ is the energy of the S_1 state, E_a and E_d are the activation energies of the ICT reaction rate constants k_a and k_d (Scheme 1), $-\Delta H$ ($= E_d - E_a$) is the difference in enthalpy between the LE and ICT states, $\tilde{\nu}^{max}$(ICT) is the energy of the maximum of the ICT fluorescence band, and δE_{FC} is the energy, relative to that of S_0, of the Franck−Condon state reached by fluorescence from the ICT state. The reaction coordinate ξ involves changes in

(48) Birks, J. B. *Photophysics of Aromatic Molecules*; Wiley: London, 1970.
(49) Zachariasse, K. A.; Busse, R.; Duveneck, G.; Kühnle, W. *J. Photochem.* **1985**, *28*, 237.
(50) Zachariasse, K. A. *Trends Photochem. Photobiol.* **1994**, *4*, 211.

Table 7. The Energy $E(S_1)$ of the S_1 State, the Activation Energies E_a and E_d of the Forward and Backward ICT Reactions (Schemes 1 and 2), the Difference in Enthalpy $-\Delta H$ between the LE and ICT States, the ICT Emission Maximum $\tilde{\nu}^{max}$(ICT) at 25 °C, and the Energy δE_{FC} of the Franck−Condon Ground State for NTC6 in Di(*n*-butyl) Ether[a]

$E(S_1)$	E_a	E_d	$-\Delta H$	$\tilde{\nu}^{max}$(ICT)	δE_{FC}
363	1	14	13	319	31

[a] All data are in kJ/mol. See Figure 8 and Scheme 2.

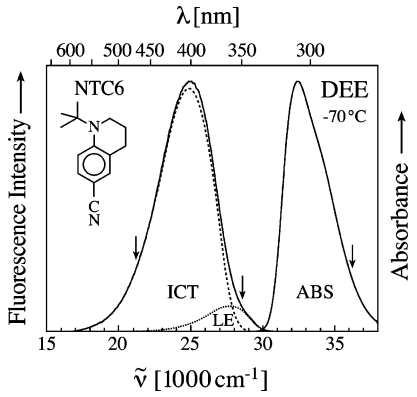

Figure 9. Fluorescence and absorption spectra at −70 °C in diethyl ether (DEE). The fluorescence spectrum consists of emissions from an LE and an ICT state. The arrows indicate the excitation (276 nm) and emission (350 and 470 nm) wavelengths used in Figure 10.

bond lengths and bond angles as well as in the orientation of solvent molecules occurring during the ICT reaction. It follows from Scheme 2 that

$$E(S_1) = -\Delta H + \tilde{\nu}^{max}(\mathrm{ICT}) + \delta E_{FC} \qquad (5)$$

By fitting the results for Φ'(ICT)/Φ(LE) in Figure 8 with eq 4, we obtained an enthalpy difference $-\Delta H$ of 13 kJ ± 1 kJ/mol, see Table 7. Inserting the data (Table 7) for $E(S_1) = 30\,380$ cm^{-1}, determined from the crossing of the absorption and fluorescence spectra, $-\Delta H = 13$ kJ/mol and $\tilde{\nu}^{max}$(ICT) = 26 700 cm^{-1} (Table 2) in eq 5, it follows that $\delta E_{FC} = 31$ kJ/mol, see Table 7. For the more flexible DMABN, δE_{FC} is considerably larger (55 kJ/mol),[11] which is the cause of the appearance of dual fluorescence with two clearly separated LE and ICT maxima, see Figure 1. The relatively small δE_{FC} value of NTC6 therefore is the reason for its strongly overlapping LE and ICT emission bands in, for example, *n*-hexane and DBE, see Figures 2 and 5.

LE and ICT Fluorescence Decays in Diethyl Ether at −70 °C. The LE and ICT fluorescence decays i_f(LE) and i_f(ICT) of NTC6 were measured in diethyl ether at −70 °C. The experiments were carried out at wavelengths at which only LE (350 nm) or only ICT (470 nm) fluorescence occurs, see the fluorescence and absorption spectra in Figure 9. A global analysis[51] of the LE and ICT fluorescence decays is presented in Figure 10. The decays are double exponential, as is to be expected with two excited species (Scheme 1). The two LE decay times are 7 ps and 8.54 ns, with relative contributions of 2% and 98%. The ICT fluorescence grows in with the same time of 7 ps, and the amplitude ratio $-A_{22}/A_{21}$ (eq 7) has a value close to unity (0.96), which means that the ICT state of NTC6 is formed from the primarily excited LE state and not by direct excitation of the ground state.[21]

From the decay times τ_2 and τ_1 together with the amplitude ratio A (eqs 6−8) and the lifetime τ_0 of a model compound, the ICT rate constants k_a and k_d and the lifetime τ_0'(ICT) can be determined,[11,21] see Table 8. The fluorescence lifetime of NIC6 in diethyl ether at −70 °C (3.09 ns) is taken for τ_0, as dual emission is not observed with this system (Figures 2 and 5).

$$i_f(\mathrm{LE}) = A_{11}\exp(-t/\tau_1) + A_{12}\exp(-t/\tau_2) \qquad (6)$$

$$i_f(\mathrm{ICT}) = A_{21}\exp(-t/\tau_1) + A_{22}\exp(-t/\tau_2) \qquad (7)$$

$$A = A_{12}/A_{11} \qquad (8)$$

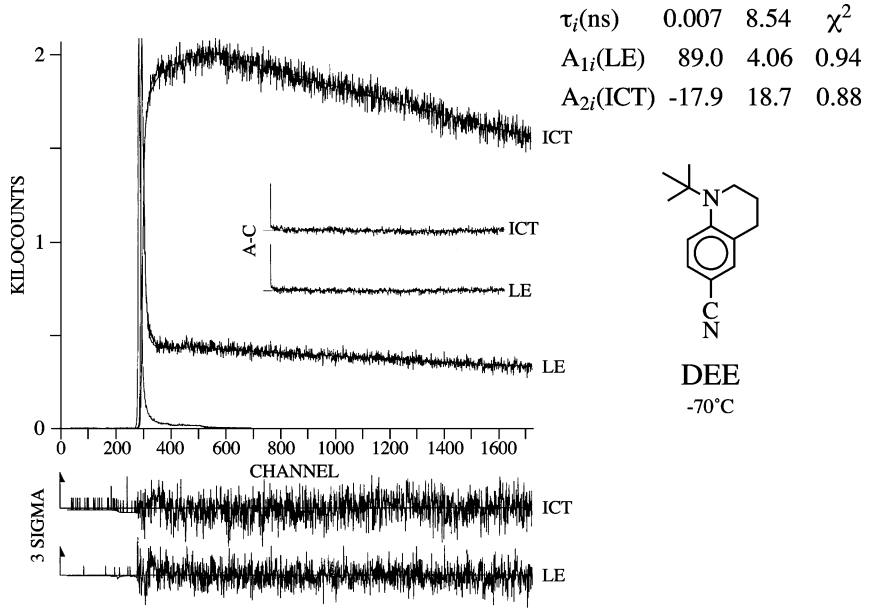

Figure 10. LE and ICT fluorescence response functions of 1-*tert*-butyl-6-cyano-1,2,3,4-tetrahydroquinoline (NTC6) in diethyl ether (DEE) at −70 °C. The LE and ICT decays are analyzed simultaneously (global analysis). The decay times (τ_2,τ_1) and their preexponential factors A_{1i} and A_{2i} are given (eqs 6−8). The weighted deviations, expressed in σ (expected deviations), the autocorrelation functions A−C, and the values for χ^2 are also indicated. Time resolution: 2 ps/chnl. Excitation wavelength: 276 nm. Emission wavelength: 350 nm (LE) and 470 nm (ICT), see Figure 9.

Table 8. Data for NTC6 in Diethyl Ether at −70 °C; Fluorescence Quantum Yields Φ(LE) and Φ′(ICT), Decay Times τ_2 and τ_1 (eqs 6 and 7) and τ_0, Amplitude Ratio A (eq 8), Rate Constants of the Forward (k_a) and Backward (k_d) ICT Reactions, ICT Fluorescence Lifetime τ_0'(ICT), and the LE and ICT Radiative Rate Constants k_f(LE) and k_f'(ICT), See Scheme 2 and Figure 10

Φ(LE)	Φ′(ICT)	Φ′(ICT)/ Φ(LE)	τ_2 [ns]	τ_1 [ns]	A	τ_0 [ns]	k_a [10^{11} s^{-1}]	k_d [10^9 s^{-1}]	τ_0'(ICT) [ns]	τ(LE/ICT)[d] [ns]	k_f(LE) [10_8 s^{-1}]	k_f'(ICT) [10_8 s^{-1}]	k_f'(ICT)/ k_f'(LE)
0.043	0.55	12.8	0.007	8.54	22	3.09[a]	1.3	5.9	9.29	0.152	1.3[b]	0.6[c]	0.53

[a] Fluorescence decay time τ_0 of NIC6 in diethyl ether at −70 °C. [b] From Φ(LE) and eq 9, see Scheme 2. [c] From Φ′(ICT) and eq 10, see Scheme 2. [d] From a deconvolution of the ICT fluorescence decay with that of LE, see text.

With $\tau_2 = 7$ ps, $\tau_1 = 8.54$ ns, $A = 21.9$, and $\tau_0 = 3.09$ ns (NIC6, Table 8), values for the rate constant k_a of 1.3×10^{11} s^{-1} and k_d of 5.9×10^9 s^{-1} are obtained. The lifetime τ_0'(ICT) equals 9.29 ns. From this analysis, $k_d + 1/\tau_0'(\text{ICT}) = 164$ ps is obtained, in good agreement with the result (153 ps) of a deconvolution of the ICT fluorescence decay with that of LE,[44,52] see Table 8. The fact that this decay time is single exponential is in accordance with the presence of two excited-state species, LE and ICT, see Scheme 1.

Radiative Rate Constants k_f(LE) and k_f'(ICT). The radiative rate constants k_f(LE) and k_f'(ICT) of NTC6 can be calculated (eqs 9 and 10) from the fluorescence quantum yields Φ(LE) and Φ′(ICT), determined in diethyl ether at −70 °C, see Table 8.

$$k_f(\text{LE}) = \Phi(\text{LE})\{1/\tau_0 + 1/\tau_0'(k_a/(k_d + 1/\tau_0'))\} \quad (9)$$

$$k_f'(\text{ICT}) = \Phi'(\text{ICT})\{1/\tau_0' + 1/\tau_0((k_d + 1/\tau_0')/k_a)\} \quad (10)$$

From these data and k_a, k_d, τ_0'(ICT), and τ_0(NIC6) (Table 8 and previous section), the following radiative rates of NTC6 in diethyl ether at −70 °C are obtained: $k_f'(\text{ICT}) = 0.59 \times 10^8$ s^{-1} and $k_f(\text{LE}) = 1.3 \times 10^8$ s^{-1}. These values are similar to those of other dual fluorescent 4-aminobenzonitriles such as DMABN.[11] Our finding that k_f'(ICT) is smaller than k_f(LE) also in the case of the planarized NTC6 indicates that the decrease in the value of the ICT radiative rate constant is not necessarily connected with an electronic decoupling of the amino and benzonitrile moieties, as postulated in the TICT model.[6−10] This decrease is attributed to the larger increase in CT character relative to the ground state of the ICT than of the LE state. This explanation is similar to that presented for the relatively small value of the radiative rate of intermolecular exciplexes $^1(A^-D^+)$.[7,53,54]

Conclusions

With the planarized tetrahydroquinoline NTC6, ICT and dual fluorescence is observed in all solvents investigated, from the nonpolar *n*-hexane to the polar acetonitrile and methanol over extended temperature ranges. This is in contrast to the observation of a single LE emission with two other tetrahydroquinolines having a methyl (NMC6) or an isopropyl (NIC6) amino substituent, as well as with the three indolines NMC5, NIC5, and NTC5. The appearance of an ICT state with a large dipole moment (19 D) in the case of NTC6 is attributed to a decrease of the energy gap $\Delta E(S_1,S_2)$, as compared with the other molecules NXC6 and NXC5. A similar reduction of $\Delta E(S_1,S_2)$ and a corresponding increase in ICT efficiency caused by the introduction of a *tert*-butyl substituent was found for tBMABN as compared with IMABN and DMABN. The observation of dual fluorescence with NTC6 shows that fast and efficient ICT is possible with aminobenzonitriles that cannot undergo a perpendicular twist and electronic decoupling of their amino group.

The results obtained here with NTC6 make clear that the absence of ICT in model compounds such as NMC6 does not mean that the ICT state of aminobenzonitriles has a TICT structure. In the aminobenzonitriles with close-lying $S_1(L_b)$ and $S_2(L_a,\text{ICT})$ states, the magnitude of $\Delta E(S_1,S_2)$ determines whether ICT does occur or not. Therefore, seemingly small modifications of the molecular structure, such as the introduction of an alicyclic ring (NMC6) or the replacement of an amino methyl substituent by hydrogen (MABN), can prevent ICT by increasing the energy gap $\Delta E(S_1,S_2)$.

Acknowledgment. The support of the Volkswagen Foundation (Project Intra- and Intermolecular Electron Transfer) is gratefully acknowledged. Dr. Attila Demeter is thanked for measuring fluorescence spectra of DIABN. We also thank Mr. Jürgen Bienert and Mr. Helmut Lesche for technical support.

Supporting Information Available: Synthetic procedures, table of solvent properties (PDF). This material is available free of charge via the Internet at http://pubs.acs.org.

JA037544W

(51) Striker, G. In *Deconvolution and Reconvolution of Analytical Signals*; Bouchy, M., Ed.; University Press: Nancy, France, 1982; p 329.
(52) Conte, J. C.; Martinho, J. M. G. *Chem. Phys. Lett.* **1987**, *134*, 350.
(53) Beens, H.; Weller, A. In *Organic Molecular Photophysics*; Birks, J. B., Ed.; Wiley: London, 1975; Vol. 2, Chapter 4.
(54) Gould, I. R.; Young, R. H.; Mueler, L. J.; Albrecht, A. C.; Farid, S. *J. Am. Chem. Soc.* **1994**, *116*, 3147.